Encapsulation in silica nanoparticles increases the phytotoxicity of essential oil from *Thymus vulgaris* in a weed species

Rym Boukhalfa[1,2*], Christian O. Dimkpa[2*], Chaoyi Deng[2], Yi Wang[2], Claudia Ruta[1], Jenny Generosa Calabrese[3], Saida Messgo-Moumene[4], Anuja Bharadwaj[2], Raja Muthuramalingam[2], Jason C. White[2], Giuseppe De Mastro[1]

[1] Department of Soil, Plant and Food Sciences (DiSSPA), University of Bari Aldo Moro, via Amendola 165/a, 70125 Bari, Italy
[2] Department of Analytical Chemistry, Connecticut Agricultural Experiment Station, New Haven, CT 06511, USA
[3] Centre for Advanced Mediterranean Agronomic Studies (CIHEAM), Via Ceglie 9, 70010 Valenzano, Bari, Italy
[4] Department of Biotechnologies, University of Blida 1, 270 Soumaa Road, Blida - Algeria

*Corresponding authors: Christian.Dimkpa@ct.gov; rymboukhalfa@yahoo.fr

Abstract

Weed control poses significant challenge to agriculture, warranting the development of effective but environmentally safe herbicides. Encapsulation of plant essential oils (EOs) with herbicidal properties in nanoscale polymers can offer high loading capacity, as well as controlled and tunable agrochemical delivery. This study investigated the use of encapsulated thyme EO against redroot pigweed (*Amaranthus retroflexus* L.), a difficult-to-control weed resistant to multiple herbicides. Three volumes of thyme EO (500, 750 and 1000 µL) were encapsulated in a silica nanoparticles (SiNPs) suspension to achieve 250 µL/mL (hereinafter ‘‘500’’), 375 µL/mL (hereinafter ‘‘750’’), and 500 µL/mL (hereinafter ‘‘1000’’) EO concentrations. The efficacies of these preparations were compared to that of pristine EO. The loading efficiencies were 26%, 42%, and 64% for the ‘‘500’’, ‘‘750’’, and ‘‘1000’’ EO preparations, respectively. TEM revealed spherical and regular SiNPs with a size range of 220-300 nm. FT-IR confirmed EO loading by the presence of characteristic peaks of isoprenoids and isomeric compounds. Herbicidal bioassays with pristine thyme EO in post-emergence treatments on *A. retroflexus* seedlings exhibited significant ($p \leq 0.05$) concentration-dependent herbicidal activity, reducing shoot biomass by 85% at the highest tested concentration (‘‘1000’’), compared to the Control (Tween 20). Encapsulation with SiNPs enhanced the herbicidal efficacy at the highest concentration by 96%. Compared to the pristine EO, EO-SiNPs also induced significant ROS production at the highest concentration, leading to cell membrane damage and imbalanced antioxidant system, as demonstrated by increased shoot malondialdehyde content (40%) and activities of the antioxidant enzymes, APX (65%), CAT (52%), and SOD (36%). These results suggest significant potential for developing an effective nano-bioherbicide using thyme EO encapsulated in SiNPs.

Key words: Herbicidal activity; thyme essential oil; silica nanoparticles; encapsulation; enhanced agrochemical delivery.

1. **Introduction**

Weed species pose a significant challenge to modern agriculture, and in conjunction with nutrient and water deficiency, causes major yield depletion and crop loss (Bindraban *et al.* 2018; Awio *et al.,* 2023). Globally, crop loss due to weed infestation is estimated at 31.5% (Kubiak *et al*., 2022), prompting the extensive use of herbicides (Qu *et al*., 2021). Glyphosate is by far the most widely applied active compound and is used in more than 750 different herbicide formulations. This large use is intensified by the spread of glyphosate-tolerant transgenic plants (Perry *et al*., 2016; Nagy *et al*., 2019). Nevertheless, widespread application of these agrochemicals causes adverse environmental impacts, significant human health concerns, and weed resistance (Taban *et al*., 2020; Mubeen *et al*., 2023). In addition to these issues are the uncertainties associated with food insecurity and climatic variabilities and extremes (Zhao *et al*., 2017). Juxtaposed with the postulation that the global population is projected to reach 9.7 billion by 2050 which warrants an increase in food production of 25%–70%, it has become critically necessary to respond to the grave issues affecting crop production (Hunter *et al*., 2017; UN, 2024).

Consequently, novel and sustainable strategies for crop protection are needed under these adverse conditions and projections. In this regard, nanotechnology has had a profound influence across various research fields, including agriculture, particularly in the development of nano-scale agrochemicals, including fertilizers, pesticides and herbicides (Adisa *et al*., 2019; Vaidya *et al.,* 2024). Nanoherbicides have demonstrated significant potential for weed control, with various types of nanoherbicides being developed utilizing both organic and inorganic nanocarriers (Takeshita *et al*., 2021; Dong *et al*., 2021; Pontes *et al*., 2021; Lima *et al*., 2021). Studies have shown that nano-enabled herbicides can offer greater efficiency and environmental advantages than conventional herbicides (Pontes *et al*., 2021; Mariana *et al*., 2022). This is due to their higher diffusion rates, improved adhesion, and longer contact time on leaf surfaces (Peixoto *et al*., 2021). Inorganic nanomaterials, such as silica, silver, and mesoporous silica nanoparticles (MSNs), are frequently used to enhance herbicidal performance by efficiently encapsulating organic molecules and providing controlled and even tunable active ingredient release (Ghazali *et al*., 2021; Mariana *et al*., 2022). Despite their increased effectiveness, the active ingredients in many nanoherbicides are often synthetic molecules that have the tendency to persist in the soil and pose environmental

hazards. Hence, there is growing interest in using natural products as active ingredients (Taban *et al*., 2020).

Aromatic plant extracts, particularly essential oils (EOs), are emerging as green alternatives to synthetic herbicides due to their beneficial properties (Li *et al*., 2023). In recent years, EOs have gained attention owing to their diverse active compounds that have shown significant potential for the control of various weed species (Araniti *et al*., 2020; El Mahdi *et al*., 2020; Zhou *et al*., 2021). These active compounds, referred to as allelochemicals, offer several advantages: they are biodegradable, generally safe for human and environmental health, and exhibit diverse modes of action (Anese *et al*., 2015). Reported mechanisms include cell injury, oxidative stress damage, DNA and RNA damage, and photosynthesis inhibition, ultimately leading to cell death (Kaur *et al*., 2021). The herbicidal mechanisms of EOs are complex, diverse, and insufficiently elucidated. However, EOs from several plant species are currently being considered for commercial herbicide products formulation. As of 2020, seven commercial bioherbicides — Matratec, GreenMatch, GreenMatchEX, WeedZap, Weed Slayer, Avenger Weed Killer, BioWeed, and WeedLock — were registered and available in the USA, Australia, and Malaysia. For example, BioWeed (Barmac, Lidcombe, Australia), Avenger Weed Killer (Avenger Products, LLC, Buford, Georgia), and Weed Slayer (Agresearch International, LLC, McKinney, United States) have been used to effectively control *Ochna serrulata* Walp., *Digitaria sanguinalis* (L.) Scop., and *Echinochloa crus-galli* (L.) P. Beauv., respectively (Travlos *et al*., 2020; Verdeguer *et al*., 2020). Notably, EOs are hydrophobic, chemically unstable, and easily degraded, all of which can complicate their use (Luo *et al*., 2022). However, nanoparticles can be used to protect EOs and enhance their stability against environmental conditions, necessitating the development of bio-nanostructured systems such as nanocapsules.

Given the well-known herbicidal potential of EOs from *Thymus* sp. pl., in the current study, a novel bio-nanoherbicide was synthesized by encapsulating the EO from *Thymus vulgaris* cultivar Varico 3 within nanoscale silica (SiNPs). The SiNP-EO formulation was characterized and then assessed for herbicidal activity on redroot pigweed (*Amaranthus retroflexus* L.). The choice of *T. vulgaris* cv. Varico 3 was motivated by its botanical and agronomic characteristics; it is a hybrid developed for a higher EO content, stability of molecules and constant production of fresh biomass.

Importantly, only few studies have explored the nanoencapsulation of EOs for herbicidal activity. The specific objectives of this study, therefore, were (i) to synthesize SiNPs and to load thyme EO into this nanocarrier; (ii) to assess the herbicidal efficacy of emulsions of pristine and SiNPs-encapsulated EO against *Amaranthus retroflexus* L.; and (iii) to determine the mechanisms of action of the synthesized nanoherbicide.

2. Materials and methods

2.1. Plant material and EO extraction and characterization

Aerial tissues of *Thymus vulgaris* cultivar Varico 3 were collected at the full flowering stage in May 2022 from the experimental farm of the University of Bari in Policoro, Basilicata, Italy. The essential oil (EO) was extracted by hydro-distillation and characterized by gas chromatography coupled with mass spectrometry in a previous study (Boukhalfa *et al*., 2024). The EO was stored at 4°C until used in the present study. The chemical composition of the EO is presented in Table 1.

Table 1. Chemical composition of *Thymus vulgaris* cultivar Varico 3 EO.

N°	Compound	KI[1]	KI[2]	Content (%)
01	α-thurjene	926	924	0.48
02	α-pinene	936	940	1.03
03	camphene	954	950	0.88
04	verbenene	967	968	0.05
05	β-pinene	979	980	0.21
06	myrcene	991	992	0.52
07	α-terpinene	1017	1012	0.13
08	p-Cymene	1022	1021	35.63
09	limonene	1029	1026	1.18
10	1,8 cineole	1031	1028	3.53
11	γ-terpinene	1059	1058	2.65
12	terpinolene	1088	1088	0.48
13	linalool	1096	1103	2.57

N°	Compound	KI[1]	KI[2]	Content (%)
14	camphor	1143	1142	1.66
15	borneol	1165	1166	1.47
16	ρ-mentha-1,5 dien-8-ol	1170	1174	1.76
17	thymol methyl ester	1235	1234	1.97
18	thymol	1290	1293	20.3
19	carvacrol	1298	1300	11,76
20	β-cedrene	1418	1404	7.69
21	caryophyllene oxide	1581	1573	5.57
Identified components (%)				100%
Monoterpene hydrocarbons				52.39
Oxygen-containing monoterpenes				38.09
Sesquiterpene hydrocarbons				4.76
Oxygen-containing sesquiterpenes				4.76
Others				--
KI: Kovats index, [1]: Literature, [2]: Calculated.				

142

143 **2.2. Synthesis of Si nanoparticles and EO-SiNPs**

144 Silica nanoparticles (SiNPs) were prepared according to Wang *et al*. (2010) with slight
145 modifications. Briefly, a mixture of 515 mmol ethanol, 33 mmol of deionized water (DI), and 32
146 mmol of ammonium hydroxide (25%) was prepared. The solution was stirred at 300 rpm while 2
147 mmol tetraethyl orthosilicate (TEOS, 98%) was gradually added as the silica source over a period
148 of 6 h. The mixture was then left to stir overnight. The resulting white precipitate was separated by
149 centrifugation for 5 cycles (2400 rpm, 5 min each at 25°C), thoroughly washed with DI water, and
150 then dried under vacuum at 75°C for 24 h. The dried SiNPs were resuspended in ethanol at 50
151 mg/mL. Subsequently, three volumes (500, 750 and 1000 µL) of thyme EO in ethanol were added
152 to the SiNPs suspension to achieve EO concentrations of 250 µL/mL (hereinafter ‘‘500’’), 375 µL
153 /mL (hereinafter ‘‘750’’), and 500 µL/mL (hereinafter ‘‘1000’’), respectively, as per Zhang *et al*.
154 (2021). The suspensions were then ultra-sonicated for 20 min and the resultant uniform suspensions
155 were allowed to incubate at ambient temperature overnight to evaporate the solvent.

2.3. Characterization of EO-SiNPs

Characterization of EO-SiNPs involved several analytical techniques to determine the zeta potential, particle size distribution, morphology, and loading efficiency of the silica nanoparticles.

Zeta Potential and Particle Size Distribution

The zeta potential and particle size distribution of the pristine (blank) SiNPs and EO-SiNPs were measured using a Malvern Zetasizer (model Nano ZS90). The electrophoretic mobility and dynamic light scattering (DLS) analyses were performed with aqueous dispersions of 0.1 g of samples in 1 mL of DI water, conducted in sextuplicate for zeta potential and in triplicate for particle size distribution.

Morphology and Particle Size Analysis

The morphology and particle size of pristine SiNPs and EO-SiNPs were determined by transmission electron microscopy (TEM). Briefly, 0.1 g of each sample was placed in 1 mL of DI water and subjected to ultrasonic treatment for 10 min to maintain particle dispersion. Subsequently, 2 µl of the aqueous particle dispersion was allowed to evaporate on a circular carbon-coated copper grid for 20 min. The samples were observed at an operating voltage of 100 kV using a Hitachi HT7800 RuliTEM (Japan).

Fourier Transform Infrared Spectroscopy (FT-IR)

The loading of EO into SiNPs was further evaluated using Fourier transform infrared spectroscopy (FT-IR, Invenio S, Bruker Co., Germany). FT-IR spectra for blank SiNPs, pristine EO, and EO-SiNPs were recorded within the range of 500–4000 cm−1 to identify characteristic absorption bands corresponding to known functional groups.

Loading Efficiency (LE%)

The loading efficiency of EO in SiNPs was determined according to Sattary *et al*. (2020). Briefly, EO-SiNPs were dispersed in 2 mL of acetonitrile, and the mixture was centrifuged at 5000 rpm for 10 min at 25°C. The absorbance of the supernatant was measured at 240 nm using a UV–Vis spectrophotometer (SpectraMax M2; Molecular Devices, Sa Jose, United States). The concentration of EO was estimated using a standard calibration curve for pristine thyme EO. The loading efficiency (LE %) was calculated using the following equation:

185

186 $$LE\ \% = (\text{Amount of loaded EO}) / (\text{Mass of loaded nanocapsules}) \times 100$$

187

188 **2.4. Biological assays**

189 **2.4.1. Assessment of the herbicidal activities of pristine EO and EO-SiNPs**

190 The herbicidal activity of freshly prepared pristine thyme EO and EO-SiNPs were tested against
191 the weed species *Amaranthus retroflexus*. Emulsions of pristine EO were prepared according to
192 Abd-El Gawad *et al*. (2020). Briefly, preparations of ‘‘500’’, ‘‘750’’, and ‘‘1000’’ EO and EO-
193 SiNPs were diluted in 2 mL Tween 20, followed by the addition of 100 mL of DI water to the
194 suspensions. Suspensions of Tween 20 and pristine SiNPs served as negative controls, while a
195 pelargonic acid-based commercially available bio-herbicide (Scythe herbicide, 57% w/w
196 pelargonic acid) was used as a positive control at a concentration coinciding with the highest EO
197 concentration in the preparations. Biological assays were conducted under greenhouse conditions
198 to evaluate the effectiveness of pristine EO and EO-SiNPs on weed seed germination and early
199 seedling growth as a post-emergent treatment. First, seed viability was assessed through a
200 germination test, where 100 seeds were sown in 90 mm Petri dishes fitted with two layers of
201 Whatman filter paper wetted with 3 mL of distilled water. The Petri dishes were sealed with
202 parafilm and placed in a controlled growth chamber maintained at 24 ± 1°C with a 16/8 h light/dark
203 cycle. After 7 days, the number of germinated seeds was counted, and the percentage of
204 germination was calculated. The effectiveness of the treatments was subsequently estimated in
205 dose-response bioassays with the weed seedlings. Specifically, to evaluate their impact on seedling
206 growth, pre-cultivation of the weed species was undertaken. Seeds were allowed to germinate in
207 the greenhouse at 22-25°C and 50-60% humidity, in nursery trays of 72 holes fitted with peat, until
208 the emergence of two true leaves. Germinated seedlings were then transplanted into pots (1000 ml)
209 filled with peat. Prior to transplanting, the pots were irrigated with water at optimal holding
210 capacity and were allowed to equilibrate and leach any excess water. The treatments were applied
211 as contact treatments by spraying with a micro-sprayer to ensure homogeneity. Each seedling
212 received 5 ml of the treatment once they reached the phenological stage of three to four true leaves,
213 corresponding to 13–14 on the BBCH scale, which is conventionally used to identify the
214 phenological development stages of plants. Treatments were applied once for the ‘‘1000’’ EO, EO-

SiNP, and the commercial herbicide preparations (5 ml x 1 application); and twice for the ‘‘750’’ and ‘‘500’’ EO and EO-SiNP preparations and the Tween 20 and SiNP controls (5 ml x 2 applications). All pots were placed in a greenhouse maintained at 22-25°C with 50-60% humidity, and were monitored daily for irrigation when necessary. All treatments and controls were replicated three times. Plants were visually evaluated for potential herbicidal effects after 24 h. At the end of this period, all plantlets were then harvested for biomass determination, cell injury assessment, and evaluation of antioxidant enzyme activities.

Cell injury indices

Several assays were conducted to evaluate the physiological impacts induced in *A. retroflexus* as a function of the treatments. To assess cell injury, lipid peroxidation levels were estimated by measuring malondialdehyde (MDA) content. Plant extraction was performed following the method of Ma *et al*. (2013). Briefly, plant samples were ground into fine powders in liquid nitrogen, and samples were extracted using a 0.1% trichloroacetic acid (TCA) solution. Subsequently, 160 µL of plant extract was mixed with 400 µL of 2% TCA and 0.5% thiobarbituric acid (TBA). The mixture was heated at 95°C for 30 min and then cooled on ice. The absorbance was measured using a UV–Vis spectrophotometer (SpectraMax M2; Molecular Devices, Sa Jose, United States) at 532 nm and 600 nm.

2.4.2. **Evaluation of total soluble protein content and antioxidant enzyme activities**

Biochemical analyses were conducted to evaluate the protein content and the activation of the enzymatic antioxidant defense system in the treated plants. The activities of three antioxidative enzymes were selected for this study, namely ascorbate peroxidase (APX), catalase (CAT), and superoxide dismutase (SOD). Enzyme extraction followed the protocols of Tamez *et al*. (2020). Briefly, plant samples were ground into fine powders in liquid nitrogen and tissues were extracted using a 25 mM potassium phosphate buffer. The protein content was determined according to the method described by Bradford (1976). APX activity was estimated based on its ability to catalyze the conversion of ascorbic acid to ascorbate and H_2O_2 (Medina-Velo *et al*., 2018). For this assay, 40 µL of enzyme extract was mixed with 228 µL of ascorbic acid and 532 µL of 0.4 mM H_2O_2. The decrease in absorbance of H_2O_2 at 290 nm was measured kinetically at 25°C during a 2-min interval using a UV–Vis spectrophotometer. CAT activity was assessed based on its ability to catalyze the decomposition of hydrogen peroxide (H_2O_2) to water (Medina-Velo *et al*., 2018). For

this assay, 40 µL of enzyme extract was mixed with 760 µL of 10 mM H_2O_2 buffer. The decrease in absorbance of H_2O_2 at 240 nm was measured kinetically at 25°C during a 3-min interval. SOD activity was determined using the photochemical reduction of nitroblue tetrazolium (NBT) method (Medina-Velo *et al*., 2018; Tamez *et al*., 2020). Briefly, 13 µL of enzyme extract was mixed with 707 µL of buffer solution containing 500 µM NBT, 78 mM L-methionine, 1.5 mM EDTA, and 100 mM potassium phosphate buffer. Eighty µL of 0.02 mM riboflavin solution was added in the dark. The solution was illuminated for 15 min in a light box, and the absorbance was measured at 560 nm using a UV–Vis spectrophotometer.

2.4.3. EO profile in treated seedlings

To confirm EO accumulation in *A. retroflexus* leaves, a phytochemical residue analysis of the main compounds in thyme essential oil was performed. After 24 h of exposure to the pristine EO and EO-SiNPs treatments, secondary metabolites were extracted from all samples (treated and negative controls) using methanol at a 1:3 (plant sample: methanol; w/v) ratio. The extraction procedure was repeated three times for each sample. The resulting extracts were pooled and filtered for chemical analysis (Vendan *et al*., 2017). Thymol, carvacrol, and p-cymene were quantified using gas chromatography-mass spectrometry (GC-MS) with an Agilent 6890N chromatography system coupled to a 5975-Mmass Spectrometry detector (Agilent Technologies, USA), employing an HP-5 MS capillary column (30 m × 0.25 mm, 0.25 µm film thickness). The GC column temperature program started at 50°C for 5 minutes, increased to 300°C at a rate of 15°C/min, and was then held at 300°C for 3 min. The injection temperature was set at 290°C, and helium was used as the carrier gas at a flow rate of 0.8 mL/min. Mass spectra were recorded in the 70 eV electron ionization mode. The EO compounds were identified by matching their retention times and mass spectra with those available in the GC-MS WILEY database.

2.5. Statistical analysis

Data obtained in these studies were statistically analyzed using Minitab® version 19.2020.1 (Minitab Software, State College, Pennsylvania, USA). A one-way analysis of variance (ANOVA) was performed to evaluate the effects of the treatments on root and shoot biomass, cell injuries, and antioxidant enzyme activities. Differences among means were assessed using Tukey's test. Statistical significance was accepted at a probability level of less than 0.05 ($p < 0.05$) (Shedden, 2015).

3. Results and Discussion

3.1. Characterization of EO-SiNPs

The morphology and size of SiNPs and EO-SiNPs were determined using TEM. The SiNPs showed a regular spherical appearance and particle size ranging between 220 and 300 nm. TEM further confirmed that the EO were successfully loaded into the SiNP. The EO was distributed in both the internal and external surfaces of SiNPs, with loading appearing to affect particle size, but not morphology (Figure 1). These results are consistent with those reported by Sattary *et al*. (2020) and Yan *et al*. (2022), who demonstrated that SiNPs and mesoporous silica nanoparticles (MSNPs) are mostly spherical and that loading of the EOs did not affect nanoparticle morphology. Interestingly, Sattary *et al*. (2020) and Yan *et al*. (2022) estimated their particle sizes to be around 50-70 nm and 100 nm, respectively. On the other hand, Attia *et al*. (2023) reported that cinnamon EO encapsulated in MSNPs were approximately 500 nm. It appears that the large disparities in particle size are modulated by the effect of the molar ratio (TEOS to NH_3) as previously noted by Prasad *et al*. (2020) as well as on the type of base used in the preparation. Indeed, while Sattary *et al*. (2020) and Yan *et al*. (2022) used sodium hydroxide, Attia *et al*. (2023) used ammonium hydroxide, as in our study.

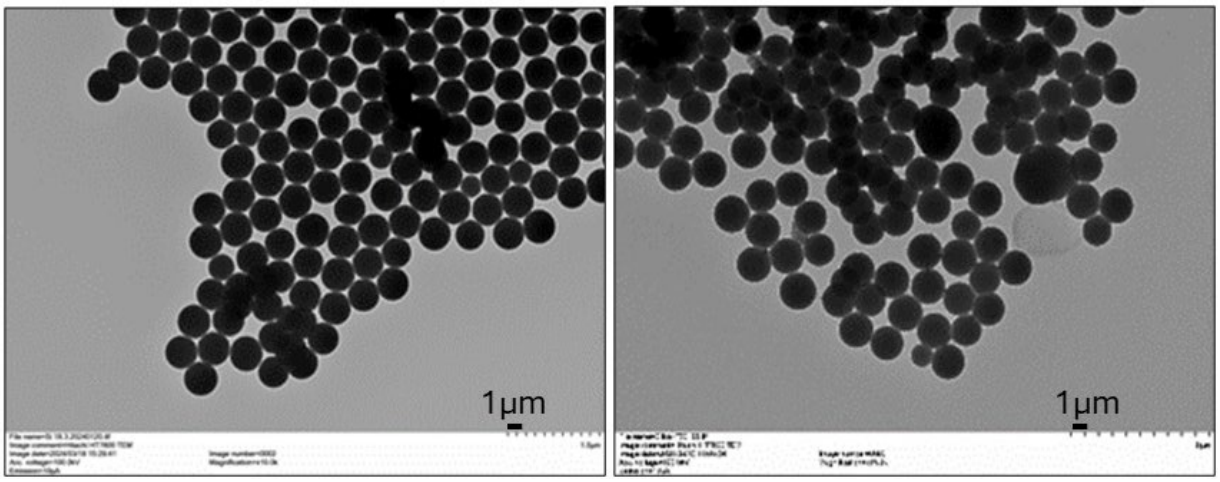

Figure 1. TEM images of SiNPs (Left) and EO-SiNPs (Right)).

Hydrodynamic diameter and zeta potential are crucial parameters in determining the availability and colloidal stability of nanosuspensions, with lower particle size often enhancing the physicochemical properties of a nanomaterial delivery system (Hasani *et al*., 2018). The particle

size distribution of pristine SiNPs and EO-SiNPs were 236.77±5.18 nm and 694.27±20.85 nm, respectively, indicating considerable size difference between the two types of materials as also indicated by TEM. These findings can be compared with those of Hasani *et al*. (2018) and Taban *et al*. (2020), who reported particle sizes ranging from 339.3 to 553.3 nm and 85.6 to 208.4 nm for different EOs encapsulated in organic polymers, including Gum Arabic, Persian gum/gelatin, and chitosan. The zeta potential for the unloaded silica was -74.00±0.38 mV, while for the EO-SiNPs it was -80.43±0.84 mV. According to Bhattacharjee *et al*. (2016), zeta potential is correlated with the stability of particle dispersions, with the following scale: 0–10 mV (highly unstable), 10–20 mV (relatively stable), 20–30 mV (moderately stable), and >30 mV (highly stable). Hence, the zeta potential analysis clearly suggested that EO-SiNPs form highly stable nanosuspensions, which is consistent with previous reports by Nithiyanantham *et al*. (2022).

FT-IR analysis shows the symmetric stretching vibration of Si-O-Si (743 cm^{-1}) and the asymmetric stretching vibration of Si-O-Si (1046 cm^{-1}) and hydroxyl groups (OH) in silica (3313 cm^{-1}) in the SiNPs spectrum, which agrees with Prasad *et al*., (2020) and Yan *et al*. (2022). The absorbance bands of the EO-loaded SiNPs were different from the pristine SiNPs. Symmetric Si-O-Si, asymmetric Si-O-Si, and O-H band stretching vibration shifted to 950 cm^{-1}, 1093 cm^{-1} and 3349 cm^{-1}, respectively. The EO-SiNPs spectrum clearly demonstrates the loading of the EO into SiNPs, with two new peaks at 802 and 941 cm^{-1}, characteristic of C–H out-of-plan bending vibration from isoprenoids and isomeric compounds like thymol, carvacrol, *p*-cymene and 1,8 cineole. In addition, for the EO-SiNPs spectrum, an overlapping of stretching vibrations of different groups was evident. These results are in line with previous studies (Topala *et al*., 2016; Moisa *et al*., 2019; Cozzolino *et al*., 2023) (Figure 2).

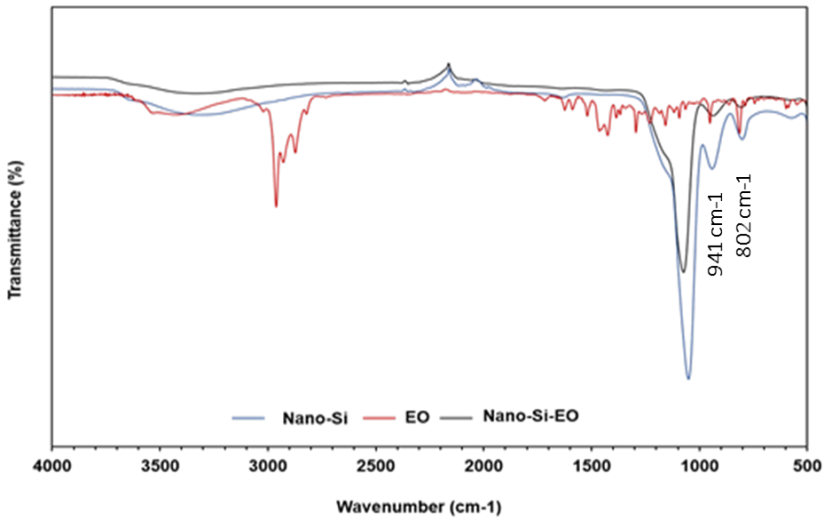

Figure 2. FT-IR spectra of pristine SiNPs (Nano-Si), EO and EO-SiNPs (Nano-Si-EO).

The loading of SiNP with EO was examined by UV-Vis spectrophotometry. LE % was obtained using a standard curve (y=0.0521x+0.0009, R^2= 0.9834). The LE analysis showed that 64% (*w*/w), 42% and 26% of EO were encapsulated in the SiNPs, respectively, for the ‘‘500’’, ‘‘750’’, and ‘‘1000’’ EO preparations. This low LE % is mainly due to the high water solubility of *p*-cymene (23.4 mg/ml) (Banerjee, 1980, in Jobdeedamrong *et al*., 2018). In this study *p*-cymene is the main components of the thyme EO.

3.2. Assessment of the herbicidal activities of pristine EO and EO-SiNPs

The herbicidal effect of pristine thyme EO and EO-SiNPs against *A. retroflexus* post-emergence was assessed in a dose-response assay. Significant damage to treated seedlings was observed after the first application with both treatments, with variability as a function of treatment type and dose. The EO-SiNPs treatment group caused the most severe necrosis in seedling shoots at 24 h, resulting in total wilting at the highest dose. A similar effect was observed in seedlings treated with pristine thyme EO at the same concentration, although the toxicity was less pronounced at lower concentrations of both materials, while no evident damage was noticed for seedlings treated with the commercial herbicide used as a positive control after 24 h of exposure (Figure 3).

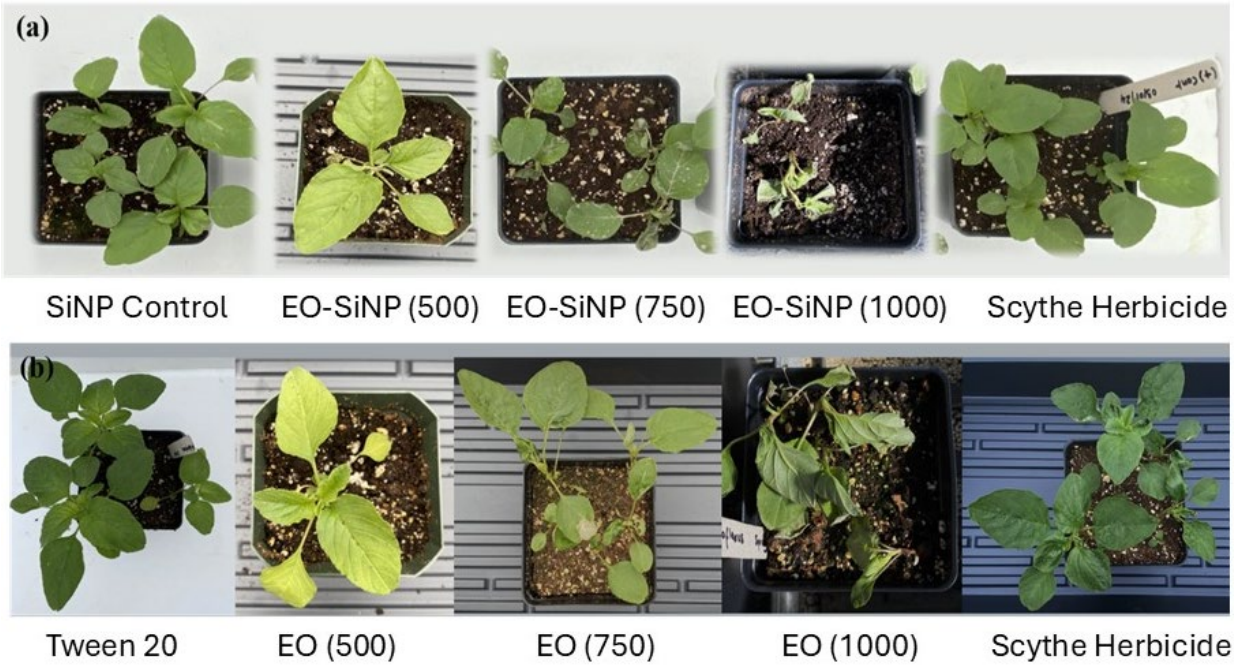

Figure 3. Photographs depicting the wilting symptoms induced by the treatments. (a): Seedlings treated with EO-SiNPs at various EO concentrations: 250 µL/mL (‘‘500’’), 375 µL/mL (‘‘750’’), and 500 µL/mL (‘‘1000’’), and a commercial herbicide (Scythe) (b): seedlings treated with Tween 20, pristine EO at various concentrations, and the commercial herbicide.

The fresh weight of *A. retroflexus* correlated with the observed necrosis symptoms as a function of treatment; both treatment groups significantly influenced shoot biomass. Specifically, exposure to the Tween 20 control resulted in an average fresh shoot biomass of 2.6 g, while the blank SiNPs increased average shoot biomass to about 6 g. However, all preparations of pristine EO (500, 750, and 1000) significantly reduced shoot biomass, compared to those negative controls. Similarly, all EO-SiNP preparations significantly reduced fresh shoot biomass, compared to the controls. However, the effects were not significantly different between the two EO types. The commercial herbicide (Scythe) used as a positive control resulted in a shoot biomass of 2.2 g. Notably, the reductions caused by the pristine EO doses were not statistically significant from the commercial herbicide result, whereas those caused by the EO-SiNPs were statistically different than the commercial herbicide at all doses. In contrast to the shoot observations, root biomass was increased by SiNPs, compared to other treatments, but was unaffected by all other treatments, relatively. This observation is likely a function of the mode of exposure (foliar) and the short treatment time (Figure 4).

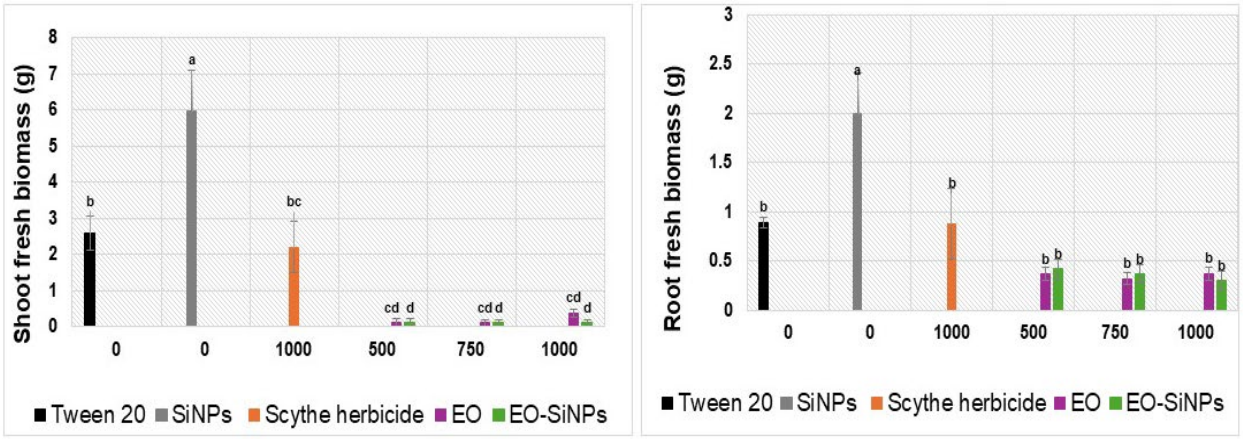

Figure 4. Effect of pristine EO and EO-SiNPs on *Amaranthus retroflexus* L. seedling fresh shoot and root biomass. Data are means and SDs of three replicates. At each dose [250 µL/mL (‘‘500’’), 375 µL/mL (‘‘750’’), and 500 µL/mL (‘‘1000’’)], bars with different letters are significantly different ($p \leq 0.05$; Tukey’s test).

These results align with current literature demonstrating the ability of thyme EOs to inhibit or reduce seed germination and seedling growth (Zhou *et al*., 2021; Miloudi *et al*., 2024; Elghobashy *et al*., 2024). However, despite the demonstrated herbicidal effect of thyme EO on *A. retroflexus*, formulating a stable EO-based bioherbicide is challenging due to their chemical characteristics, particularly high volatility. Therefore, encapsulation of EO is proposed as a solution to preserve its efficacy and control the release of secondary metabolites (Maes *et al*., 2019). The results obtained in this study regarding the use of a nano-carrier for EO delivery as a bioherbicide are promising. EO-SiNPs enhanced the efficacy of thyme EO, causing more severe wilting and necrotic symptoms in *A. retroflexus*. To the best of our knowledge, the use of polymers as nano-carriers for the delivery of essential oils for herbicidal purposes is limited to a small number of studies. Our results align with those reported by Taban *et al*. (2020), who demonstrated that nano-encapsulated *Satureja hortensis* L. EO in Gum Arabic, Persian gum/gelatin, and Persian gum developed via crosslinking with citric acid and transglutaminase was phytotoxic to *A. retroflexus,* by 33-233% as a post-emergence treatment, compared to the surfactant, Tween 80. Unfortunately, no non-nanoencapsulated EO treatment was evaluated in that study. Similarly, Alipour *et al*. (2019) and Synowiec *et al*. (2020) reported enhanced herbicidal efficiency of microencapsulated EOs of *Rosmarinus officinalis* L. and *Carum carvi* L. using starch and maltodextrin, respectively, as the

biopolymer carriers. These treatments were incorporated into the soil as pre-emergence applications.

3.3. Cell injury indices

The Tween 20 and SiNP control treatments had MDA levels of 0.81 and 0.85 mM/g^{-1}, respectively. Both pristine EO and EO-SiNPs significantly increased MDA content in the shoots and roots of treated *A. retroflexus* seedlings, compared to the controls (Figure 5). In shoots, the MDA content increased with dose, with encapsulated EO showing a statistically stronger effect than the pristine EO across all concentrations. At the lowest EO and EO-SiNPs concentration (500), MDA content was nearly identical to the positive control (Scythe), measuring 2.4 ± 0.2, 1.7 ± 0.2, and 2.4 ± 0.3 mM/g^{-1} for EO-SiNPs, pristine EO, and the positive control, respectively, while the MDA contents in the negative controls were lower than 1 mM/g^{-1}. In contrast, at the highest concentration (1000), the MDA content was approximately 7.3 ± 0.25 mM/g^{-1} for EO-SiNPs and 5.2 ± 0.25 mM/g^{-1} for the pristine EO. Compared to the commercial herbicide (Scythe), shoot MDA level was significantly increased by the 700 and 1000 EO and EO-SiNP preparations (Figure 5). In the roots, the Tween 20 and SiNP control treatments had MDA levels of 0.75 mM/g^{-1} apiece. As with the shoot, both types of EO treatment significantly increased MDA content in a dose-dependent manner in the root. EO-SiNPs also demonstrated superior efficacy in this case. With the 1000 preparation, root MDA content was 2.2 ± 0.06 mM/g^{-1} for EO-SiNPs and 1.5 ± 0.09 mM/g^{-1} for the pristine EO. With the 500 preparation, both treatments outperformed the positive control (Scythe), thus highlighting the potentially enhanced herbicidal potential of thyme EO even at lower concentrations. This increase in MDA content indicates that both treatments promoted lipid peroxidation, causing significant damage to the cell membrane integrity of *A. retroflexus*, with EO-SiNPs being more effective. Importantly, direct shoot exposure with the treatments resulted in root damage at the cellular level, suggesting subtle systemic effects.

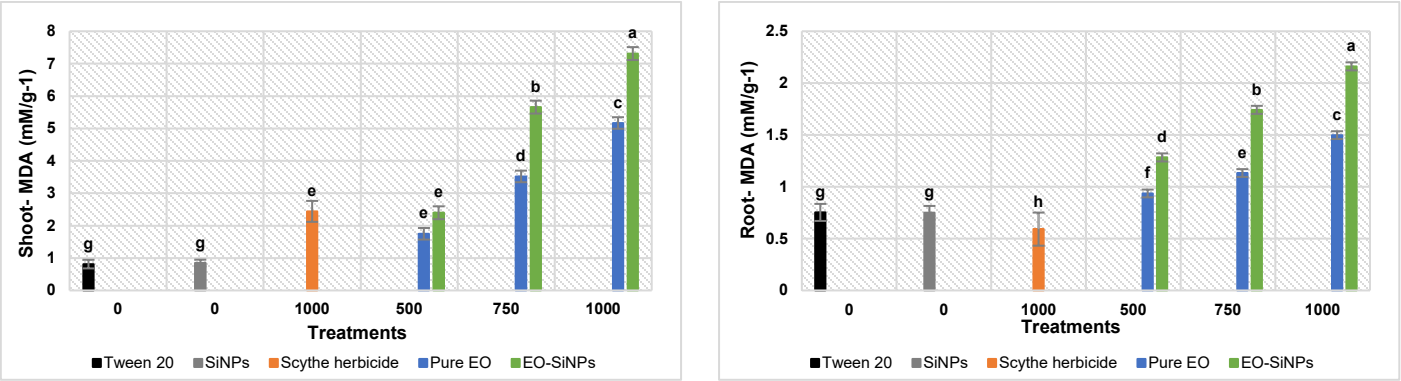

Figure 5. Effect of pristine EO and EO-NanoSi on malondialdehyde (MDA) content of *A. retroflexus* shoot and root tissues. Data are means and SDs of nine replicates. At each dose [250 µL/mL (‘‘500’’), 375 µL/mL (‘‘750’’), and 500 µL/mL (‘‘1000’’)], bars with different letters are significantly different ($p \leq 0.05$; Tukey’s test).

The finding of MDA alterations by EO-SiNP is consistent with the results of Alipour *et al*. (2019), Synowiec *et al*. (2020), and Taban *et al*. (2020), who observed that their treatments with different encapsulating materials increased MDA content, while decreasing total chlorophyll, phenolic, and flavonoid contents in *A. retroflexus* and *R. sativus* relative to the biopolymer free controls. According to Lins *et al*. (2019), the molecular structure of each EO component may have its own specific mode of action. The herbicidal effect observed in our study could be attributed to the presence of oxygenated monoterpenes, such as thymol, carvacrol, and p-cymene, which have been shown to significantly impact weed germination and growth (Grulová *et al*., 2020; Verdeguer *et al*., 2020; De Oliveira *et al*., 2023). It is worth highlighting that the main compounds of the thyme EO used in this study are thymol, carvacrol, and p-cymene, which further confirms the herbicidal potential of thyme EO. Araniti *et al*. (2020) demonstrated that the terpenic phenol thymol significantly altered the plant water status, increased abscisic acid content, induced stomatal closure, and caused heat accumulation in the leaf lamina. These changes resulted in significant accumulation of ROS and damage to the photosynthetic machinery. Chaimovitsh *et al*. (2016) and Zhang *et al*. (2021) found that carvacrol increased electrolyte leakage and MDA formation in *Arabidopsis thaliana* and *Spinacia oleracea*, respectively, when studying the herbicidal effects of monoterpenes and carvacrol Notably, the latter study involved carvacrol nanoemulsion. The elevated MDA content noted in the current study reflected the leaf damage and necrosis observed during the greenhouse experiments, consistent with previous reports on allelochemicals, mainly terpenoids. These chemicals alter membrane permeability and polarization, leading to electrolyte

436 leakage and lipid peroxidation, causing cell content leakage and resulting in slowed plant growth
437 or death (Andriana *et al*., 2018; Scavo *et al*., 2019; M'barek *et al*., 2019; Pouresmaeil *et al*., 2020).
438
439 **3.4. Evaluation of total soluble protein content and antioxidant enzyme activities**
440 The total protein content and antioxidant enzymes (APX, CAT, and SOD) activities in both shoot
441 and root of *A. retroflexus* were evaluated to understand the physiological mechanisms underlying
442 the herbicidal activity of pristine thyme EO and its encapsulated form. The protein content was
443 significantly affected by the treatments in a dose dependent fashion, as compared to the Tween 20
444 (0.3 and 0.2 µg, for the shoot and root) and SiNP (0.7 and 0.2 µg, for the shoot and root) controls
445 (Figure 6). The total soluble protein content increased significantly in the treated seedlings,
446 compared to the controls. Pristine EO, and more so EO-SiNPs, showed the highest protein content
447 in the shoots with the 1000 preparations, where EO-SiNPs induced 1.8 ± 0.3 µg proteins in the
448 shoots, significantly differing from the 1.5 ± 0.2 µg recorded for the pristine EO. In the roots, the
449 protein content was 1.6 ± 0.1 µg for EO-SiNPs, which also differed significantly from the 0.6 ±
450 0.2 µg obtained for pristine EO. Notably, shoot protein content was not affected by EO, compared
451 to the commercial herbicide; however, the EO-SiNP 750 and 1000 preparations significantly
452 increased the protein levels, relative to the commercial herbicide product These outcomes were
453 similar for the root, except in the case of EO 1000 (Figure 6).
454
455 In the shoot of *A. retroflexus*, APX, CAT, and SOD activities from the Tween 20 and SiNP control
456 treatments were 0.3 and 0.7 units APX/mg protein; 0.7 units CAT/mg protein apiece; and 4.9 and
457 4.8 SOD units/mg FW, respectively. In the root, these values were 0.1 and 0.3 units APX/mg
458 protein; 0.6 and 0.4 units CAT/mg protein; and 2.9 and 2.6 SOD units/mg FW, respectively, for
459 Tween 20 and SiNP. Notably, APX, CAT, and SOD responded strongly to treatment with pristine
460 thyme EO and EO-SiNPs. The enzyme activities were significantly enhanced and maintained at
461 high levels in both shoot and root under both thyme EO and EO-SiNPs exposures at all doses,
462 relative to the above control treatments (Figure 6). Remarkably, EO-SiNPs caused significantly
463 greater response than EO in both plant tissues. With regards to the commercial herbicide, a shoot
464 APX activity of 2.1 units /mg protein was recorded, which in comparison was significantly
465 increased only by the EO 1000 preparation, but more strongly so by EO-SiNP preparation at all the
466 concentrations. The commercial herbicide had a shoot CAT activity of 1.1 units/mg protein, which

in comparison was significantly increased by EO 750 and 1000; and by all treatments of EO-SiNPs. Similarly, the shoot SOD activity of 5.4 units/mg FW caused by the commercial herbicide was in comparison significantly increased by EO 750 and 1000, and by all treatments of EO-SiNPs. In the root, the commercial herbicide had an APX activity of 0.3 units /mg protein, a CAT activity of 0.7 units /mg protein, and a SOD activity of 3.7 units/mg FW. Notably, all EO and EO-SiNP treatments significantly increased these enzyme activities (Figure 6). Taken together, these results suggest that both pristine thyme EO and EO-SiNPs induced significant abiotic stress in *A. retroflexus* seedlings within 24 h, activating the antioxidant defense systems for reactive oxygen species scavenging. Importantly, EO-SiNPs exerted the greatest phytotoxic effect.

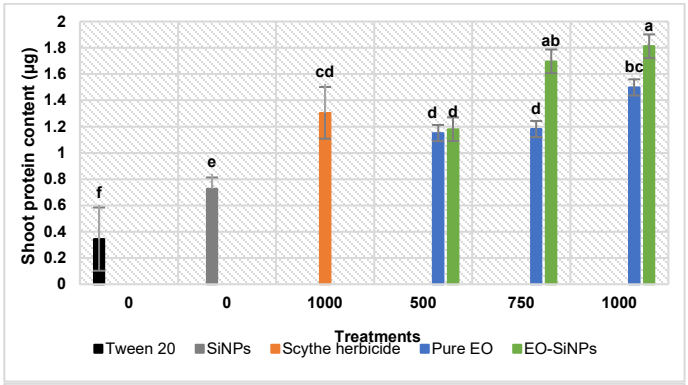

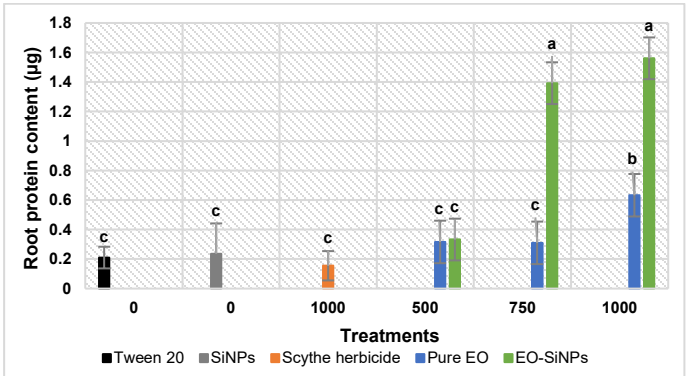

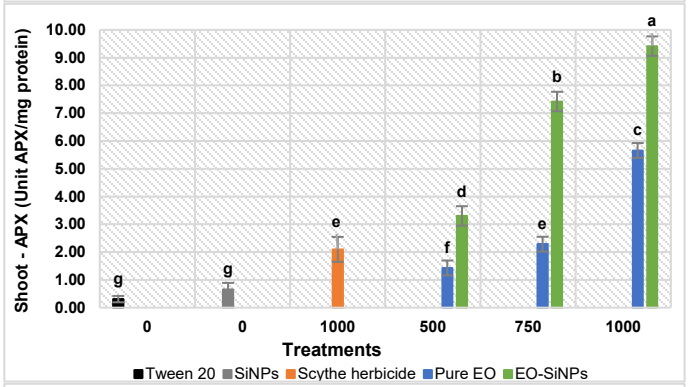

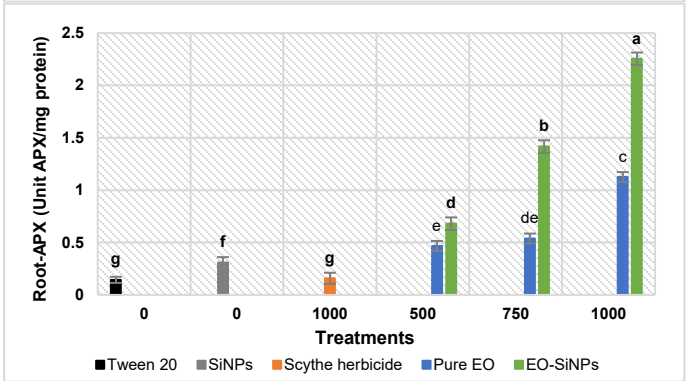

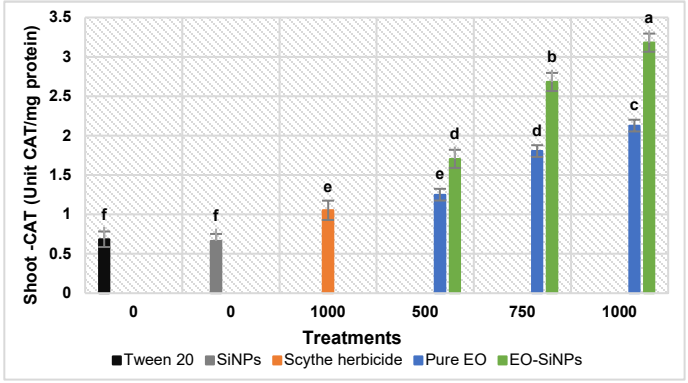

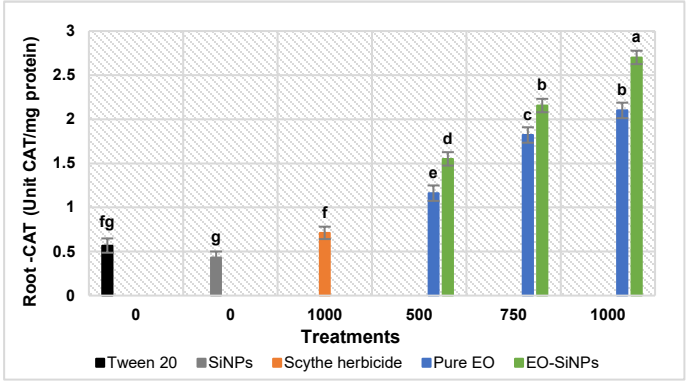

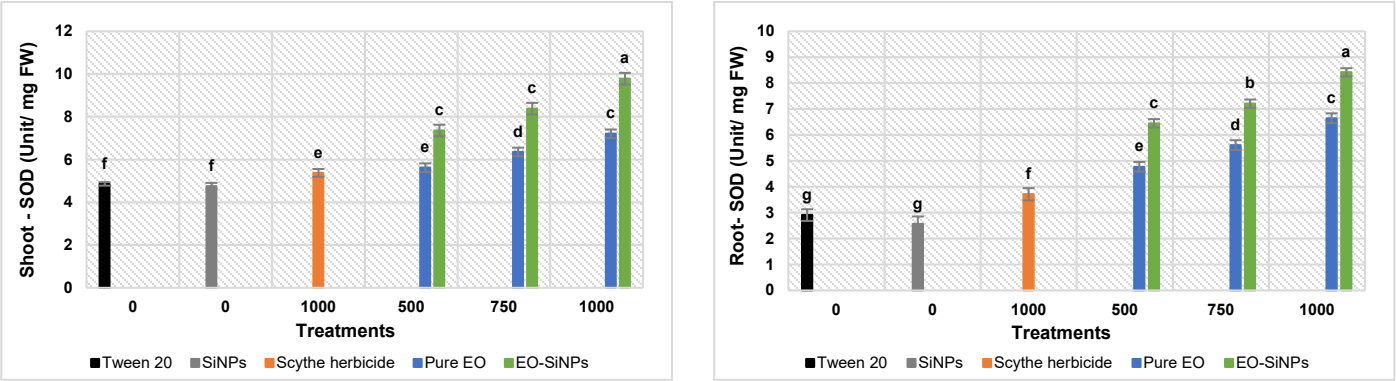

Figure 6. Effect of pristine EO and EO-SiNPs on total protein content and antioxidant enzyme (APX, CAT, and SOD) activities in shoots and roots of *A. retroflexus* seedlings. Data are means and SDs of nine replicates. At each dose [250 µL/mL (‘‘500’’), 375 µL/mL (‘‘750’’), and 500 µL/mL (‘‘1000’’)], bars with different letters are significantly different ($p \leq 0.05$, Tukey’s test).

Together, these data demonstrated that EO-SiNPs significantly affected the defense mechanisms of *A. retroflexus*, causing more severe damage than pristine EO. Previous reports have noted similar biochemical and metabolic disturbances in weed species following the application of EO-based treatments (Pouresmaeil *et al*., 2020; Han *et al*., 2021; Li *et al*., 2023). Here, pristine thyme EO and its nanoformulation induced a generalized increase in protein content and activated the antioxidant enzyme activities (APX, CAT, and SOD) in the shoots and roots of the seedlings. Taban *et al*. (2020), previously observed that treatments with different encapsulating materials increased POD enzyme activity to prevent accumulation of H_2O_2. Together, these findings indicate that the treatments triggered intense ROS production in both shoots and roots, activating the plant's defense mechanisms, particularly through increased antioxidant enzyme activity for ROS scavenging and oxidative stress mitigation. Upon recognizing the stressful condition, one of the earliest plant defense responses is the production of ROS, including singlet oxygen (O), superoxide (O–), hydrogen peroxide (H_2O_2), and hydroxyl radicals (OH−) (Zaid *et al*., 2019). Although ROS are constantly produced during aerobic metabolic reactions, their levels increase in response to stress (Ali *et al*., 2018). The APX data from the current study suggests that the treatments primarily affected the membrane integrity of the plant cells, as APX significantly increased in response to the treatments. APX has a high affinity for H_2O_2 detoxification, playing a crucial role in removing

H_2O_2 and maintaining ROS levels inside the cell. The results for CAT suggest that the treatments moderately impacted the photorespiration system, as Class I catalases, predominant in photosynthetic tissues, are involved in scavenging H_2O_2 produced during photorespiration. Overall, the inhibitory mechanisms of thyme EO are like those of EOs from other plants, though their main targets remain unclear. Commercial herbicides are generally classified into different categories based on their mode of action and active targets, such as HPPD inhibitors, ALS inhibitors, PPO inhibitors, and ACCase inhibitors. Given the mode of action of the main thyme EO compounds and the evaluation results of the physiological mechanisms underlying its herbicidal activity, it appears that thyme EO is like PPO inhibitors. Protoporphyrinogen oxidase (PPO) inhibitors are primarily contact-type and post-emergence herbicides that disrupt cell membranes by inhibiting the PPO enzyme located in the outer envelope of chloroplasts. This inhibition causes the colorless protoporphyrinogen (protogen) precursor to leak into the cytoplasm, where it is converted into photodynamic protoporphyrin IX (proto). In the presence of light, proto generates a burst of ROS that react with membrane lipids, leading to lipid peroxidation and subsequent cell death (Barker *et al*., 2023). In their study on the role of antioxidants in protecting plants against PPO inhibitors, Dayan *et al*. (2019) noted that increases in certain antioxidants, particularly hydrophilic antioxidants such as reduced glutathione and ascorbic acid (ascorbate), were induced in response to this stress. Conversely, the addition of buthionine sulfoximine, which inhibits glutathione biosynthesis, made plants more sensitive to acifluorfen-methyl. These reducing agents protect plants by quenching ROS generated by the photoactivation of proto, with ascorbate and reduced glutathione providing superior protection against superoxide compared to hydrogen peroxide quenching by ascorbate. This aligns with our findings, as we observed significant SOD activity, suggesting that the plant primarily activated both APX and SOD for ROS scavenging and preserving cell integrity. Notably, encapsulation of EO with SiNPs heightened these enzyme activities likely due to improved active ingredient delivery, thereby potentiating the role of materials engineering in modulating plant biochemical responses to enhance sustainable agriculture.

3.5. Profiling of pristine EO and EO-NanoSi compounds in treated seedlings

GC-MS analysis of the shoots to characterize the EO profile was completed (Table 2). A considerable amount of thymol residue was detected in *A. retroflexus* treated with pristine EO and EO-SiNPs, whereas carvacrol and *p*-cymene were below the analytical detection limits. This

indicates that the treatments were able to penetrate the cuticle of the plant leaves, likely the result of the polar surface area of each these phytochemicals (Vendan *et al*., 2017). Because of a lack of shoot tissues due to severe tissue damage, it was not possible to assess the residues of the seedlings treated with EO-SiNPs 1000. Nevertheless, the results of this study, along with the proposed modes of action, were further supported by the profiling of the main active compounds of thyme EO. Thymol residues in the plant extract confirm the successful penetration of the treatments into the cells and demonstrate that SiNPs can be an effective carrier for thyme EO delivery and potentially other agrochemical cargo.

Table 2. Thymol residues detected in *A. retroflexus* shoot extracts following treatments with EO and EO-SiNP.

	Residue (µg/g)		
Treatment	500	750	1000
Pristine EO	1.6	5.1	15.9
EO-SiNPs	1.2	5.5	--

4. Conclusions

Thyme essential oil (EO) was successfully loaded into silica nanoparticles (SiNPs) to produce a nano-bioherbicide. TEM, zeta potential, particle size distribution, FT-IR, and UV-Vis analyses together confirmed the successful encapsulation of the EO into SiNPs. When used as a post-emergence treatment, thyme EO demonstrated strong herbicidal activity. Encapsulating the EO in SiNPs showed a tendency to enhance its toxicity, especially at the highest concentration. Mechanistically, EO-SiNPs caused severe necrosis in seedlings, adversely affecting plant physiological processes. The treatment increased protein and malondialdehyde content, as well as APX, CAT and SOD enzyme activities, indicating significant reactive oxygen species production and oxidative stress in the weed plant. The results suggest membrane system leakage and considerable oxidative damage to plant cells, implicating protoporphyrinogen oxidase as a potential target for thyme EO. Although Si is known to provoke plant metabolic responses under different conditions (Sarita *et al.* 2024), taken together, our data strongly indicate that all the observed effects were not contributed to by the SiNP. Rather, the EO was responsible for the herbicidal effects that, however, were significantly accentuated by encapsulation with SiNP. These findings, therefore, provide evidence for the potential use of EO-SiNPs as an effective bioherbicide. Though EOs can

control weeds, they suffer from high instability, making their long-term storage a major concern. By formulating EO encapsulated with SiNP, the chance of improving EO stability is greater, alongside enhanced active ingredient release and herbicidal efficacy. To this end, further studies to optimize loading efficiency, understand EO release and product stability over time, assess the formulation against a wide range of weed species and food crops, and omic studies to better understand the mechanisms of action, are being envisaged.

Acknowledgement

This work has been supported by the International Centre for Advanced Mediterranean Agronomic Studies- Mediterranean Agronomic Institute of Bari (CIHEAM-IAM Bari- Italy). Portions of this work was supported by the NSF Center for Sustainable Nanotechnology under grant number CHE-2001611; The NSF CSN is part of the Center for Chemical Innovation Program." Many thanks to the Connecticut Agricultural Experiment Station's Department of Analytical Chemistry staff for various assistances provided during this study.

Competing Interest: The authors declare no competing interests in this work

References

Abd-El Gawad, A.M., El Gendy, A.E.-N.G., Assaeed, A.M., Al-Rowaily, S.L., Alharth, A.S., Mohamed, T.A., Nassar, M.I., Dewir, Y.H., Elshamy, A.I., 2021. Phytotoxic effects of plant essential oils: A systematic review and structure-activity relationship based on chemometric analyses. Plants 10, 36. https://doi.org/10.3390/plants10010036.

Adisa, I.O., Pullagurala, V.L.R., Peralta-Videa, J.R., Dimkpa, C.O., Elmer, W.H., Gardea-Torresdey, J.L., White, J.C., 2019. Recent advances in nano-enabled fertilizers and pesticides: A critical review of mechanisms of action. Environ. Sci. Nano **6,** 2002-2030. https://doi.org/10.1039/C9EN00265K.

Alipour, M., Saharkhiz, M.J., Niakousari, M., Damyeh, M.S., 2019. Phytotoxicity of encapsulated essential oil of rosemary on germination and morphophysiological features of amaranth and radish seedlings. Scientia Horticulturae 243, 131-139. https://doi.org/10.1016/j.scienta.2018.08.023.

590 Amato, G., Caputo, L., Francolino, R., Martino, M., De Feo, V., De Martino, L., 2023. *Origanum*
591 *heracleoticum* essential oils: chemical composition, phytotoxic and alpha-amylase inhibitory
592 activities. Plants 12(4), 866. https://doi.org/10.3390/plants12040866.
593 Andriana, Y., Xuan, T.D., Quan, N.V., Quy, T.N., 2018. Allelopathic potential of *Tridax*
594 *procumbens* L. on radish and identification of allelochemicals. Allelopathy J. 43, 223–238.
595 https://doi.org/10.26651/allelo.j./2018-43-2-1143.
596 Anese, S., Jatoba, L.J., Grisi, P.U., Gualtieri, S.C.J., Santos, M.F.C., Berlinck, R.G.S., 2015.
597 Bioherbicidal activity of drimane sesquiterpenes from *Drimys brasiliensis* Miers roots. Ind.
598 Crop. Prod. 74, 28–35. https://doi.org/10.1016/j.indcrop.2015.04.042.
599 Araniti, F., Miras-Moreno, B., Lucini, L., Landi, M., Abenavoli, M.R., 2020. Metabolomic,
600 proteomic and physiological insights into the potential mode of action of thymol, a phytotoxic
601 natural monoterpenoid phenol. Plant Physio. Biochem. 153, 141-153.
602 https://doi.org/10.1016/j.plaphy.2020.05.008.
603 Attia, R.G., Khalil, M.M.H., Hussein, M.A., Fattah, H.M.A., Rizk, S.A., Ma'moun, S.A.M., 2023.
604 Cinnamon oil encapsulated with silica nanoparticles: chemical characterization and evaluation
605 of insecticidal activity against the Rice Moth, *Corcyra cephalonica*. Neotrop. Entomol. 52,
606 500-511. https://doi.org/10.1007/s13744-023-01037-1.
607 Awio, T., Struik, P.C., Senthilkumar, K., Dimkpa, C.O., Otim-Nape, G.W., Stomph, T.J., 2023.
608 Indigenous nutrient supply, weeding and fertilisation strategies influence on-farm N, P and K
609 use efficiency in lowland rice. Nutr. Cycl. Agroecosys. 126, 163–
610 180. https://doi.org/10.1007/s10705-023-10275-z.
611 Barker, A.L., Pawlak, J., Duke, S.O., Beffa, R., Tranel, P.J., Wuerffel, J., Young, B., Porri, A.,
612 Liebl, R., Aponte, R. and Findley, D., 2023. Discovery, mode of action, resistance mechanisms,
613 and plan of action for sustainable use of Group 14 herbicides. Weed Sci. 71(3), 173-188.
614 https://doi.org/10.1017/wsc.2023.15.
615 Bhattacharjee, S., 2016. DLS and zeta potential–what they are and what they are not? J. controlled
616 release 235, 337-351. https://doi.org/10.1016/j.jconrel.2016.06.017.
617 Bindraban, P.S., Dimkpa, C.O., Angle, S., Rabbinge, R., 2018. Unlocking the multiple public good
618 services from balanced fertilizers. Food Sec. 10, 273-285. https://doi.org/10.1007/s12571-018-
619 0769-4
620

Boukhalfa, R., Ruta, C., Messgo-Moumene, S., Calabrese, G., Argentieri, M.P., De Mastro, G., 2024. Valorization of Mediterranean species of thyme for the formulation of bio-herbicides. *Agronomy*. 3146404.

Bradford, M. 1976. A rapid and sensitive method for the quantification of microgram quantities of protein utilizing the principal of protein-dye binding. Anal. biochem. 72 (1-2), 248-254. https://doi.org/10.1006/abio.1976.9999.

Casella, F., Vurro, M., Valerio, F., Perrino, E.V., Mezzapesa, G.N., Boari A., 2023. Phytotoxic effects of essential oils from six *Lamiaceae* species. Agronomy 13(1), 257. https://doi.org/10.3390/agronomy13010257.

Chaimovitsh, D., Shachter, A., Abu-Abied, M., Rubin, B., Sadot, E., Dudai, N., 2017. Herbicidal activity of monoterpenes is associated with disruption of microtubule functionality and membrane integrity. Weed Sci. 65, 19–30. https://doi.org/10.1614/WS-D-16-00044.1.

Dayan, F.E., Barker, A., Dayan, L., Ravet, K., 2019. The role of antioxidants in the protection of plants against inhibitors of protoporphyrinogen oxidase. Reactive Oxygen Species 7(19), 55-63. http://dx.doi.org/10.20455/ros.2019.811

de Oliveira Roberto, C.E., Pinheiro, P.F., de Assis Alves, T., da Silva, J.A., Praça-Fontes, M.M., Soares, T.C.B., 2023. Phytogenotoxicity of thymol and semisynthetic thymoxyacetic acid in pre/post emergence of model plants and weeds. Environ. Sci. Pollut. Res. 30(13), 38955-38969. https://doi.org/10.1007/s11356-022-24753-4.

Dong, J., Liu, X., Chen, Y., Yang, W., Du, X., 2021. User-safe and efficient chitosan-gated porous carbon nanopesticides and nanoherbicides. J. Colloid Interface Sci. 594, 20–34. https://doi.org/10.1016/j.jcis.2021.03.001.

Dvořák, P., Krasylenko, Y., Zeiner, A., Šamaj, J., Takáč, T., 2021. Signaling toward reactive oxygen species-scavenging enzymes in plants. Front. Plant Sci. 11, 618835. https://doi.org/10.3389/fpls.2020.618835.

Elghobashy, R.M., El-Darier, S.M., Atia, A.M., Zakaria, M., 2024. Allelopathic potential of aqueous extracts and essential oils of *Rosmarinus officinalis* L. and *Thymus vulgaris* L. J. Soil Sci. Plant Nut. 24(1), 700-715. https://doi.org/10.1007/s42729-023-01576-x.

El Mahdi, J., Tarraf, W., Ruta, C., Piscitelli, L., Aly, A., De Mastro, G., 2020. Bio-herbicidal potential of the essential oils from different *Rosmarinus officinalis* L. chemotypes in laboratory assays. Agronomy 10(6), 775. https://doi.org/10.3390/agronomy10060775.

652 Forini, M.M., Pontes, M.S., Antunes, D.R., de Lima, P.H., Santos, J.S., Santiago, E.F., Grillo, R.,
653 2022. Nano-enabled weed management in agriculture: From strategic design to enhanced
654 herbicidal activity. Plant Nano Bio. 1, 100008. https://doi.org/10.1016/j.plana.2022.100008.
655 Ghazali, S.A.I.S.M., Fatimah, I., Bohari, F.L., 2021. Synthesis of hybrid organic-inorganic
656 hydrotalcite-like materials intercalated with duplex herbicides: The characterization and
657 simultaneous release properties. Molecules 26, 5086.
658 https://doi.org/10.3390/molecules26165086.
659 Gruľová, D., Caputo, L., Elshafie, H.S., Baranová, B., De Martino, L., Sedlák, V., Gogaľová, Z.,
660 Poráčová, J., Camele, I., De Feo, V., 2020. Thymol chemotype *Origanum vulgare* L. essential
661 oil as a potential selective bio-based herbicide on monocot plant species. Molecules 25(3), 595.
662 https://doi.org/10.3390/molecules25030595.
663 Han, C., Shao, H., Zhou, S., Mei, Y., Cheng, Z., Huang, L., Lv, G., 2021. Chemical composition
664 and phytotoxicity of essential oil from invasive plant, *Ambrosia artemisiifolia* L. Ecotoxico.
665 Environ. Saf. 211, 111879. https://doi.org/10.1016/j.ecoenv.2020.111879.
666 Hasani, S., Ojagh, S.M., Ghorbani, M., 2018. Nanoencapsulation of lemon essential oil in
667 Chitosan-Hicap system. Part 1: study on its physical and structural characteristics. Int. J. Biol.
668 Macromol. 115, 143–151. https://doi.org/10.1016/j.ijbiomac.2018.04.038.
669 Hunter, M.C., Smith, R.G., Schipanski, M.E., Atwood, L.W., Mortensen, D. A., 2017. Agriculture
670 in 2050: Recalibrating targets for sustainable intensification. BioSci. 67(4), 386–391.
671 https://doi.org/10.1093/biosci/bix010.
672 Jobdeedamrong, A., Jenjob, R., Crespy, D., 2018. Encapsulation and release of essential oils in
673 functional silica nanocontainers. Langmuir 34(44), 13235-13243.
674 https://doi.org/10.1021/acs.langmuir.8b01652.
675 Kaur, P., Gupta, S., Kaur, K., Kaur, N., Kumar, R., Bhullar, M.S., 2021. Nanoemulsion of
676 *Foeniculum vulgare* essential oil: a propitious striver against weeds of *Triticum aestivum*. Ind
677 Crops Prod. 168:113601. https://doi.org/10.1016/j. indcrop.2021.113601.
678 Kubiak, A., Wolna-Maruwka, A., Niewiadomska, A., Pilarska, A.A., 2022. The problem of weed
679 infestation of agricultural plantations vs. the assumptions of the European biodiversity strategy.
680 Agronomy 12, 1808. https://doi.org/10.3390/agronomy12081808.

Li, J., Chen, H., Guo, C., Chen, Q., Zhao, T., Chen, X., Du, Y., Du, H., Miao, Y. and Liu, D., 2023. *Artemisia argyi* essential oil exerts herbicidal activity by inhibiting photosynthesis and causing oxidative damage. Ind. Crops Prod. 194, 116258. https://doi.org/10.1016/j.indcrop.2023.116258.

Lima, P.H.C., Antunes, D.R., Forini, M.Md.L., Pontes, Md.S., Mattos, B.D., Grillo, R., 2021. Recent advances on lignocellulosic-based nanopesticides for agricultural applications. Front. Nanotechnol. 3, 809329. https://doi.org/10.3389/fnano.2021.809329.

Luo, Y., Su, J., Guo, S., Cao, Z., Liu, Z., Wu, S., Mao, Y., Zheng, Y., Shen, W., Li, T., Ge, X., 2022. Preparation of humidity-responsive cinnamon essential oil nanomicelles and its effect on postharvest quality of strawberries. Food Bioprocess Techno. 15(12), 2723–2736. https://doi.org/10.1007/s11947-022-02906-0

M'barek, K., Zribi, I., Ullah, M.J., Haouala, R., 2019. The mode of action of allelochemicals aqueous leaf extracts of some *Cupressaceae* species on lettuce. Sci. Hortic. 252, 29–37. https://doi.org/10.1016/j.scienta.2019.03.009.

Ma, C., Chhikara, S., Xing, B., Musante, C., White, J.C., Dhankher, O.P., 2013. Physiological and molecular response of *Arabidopsis thaliana* (L.) to nanoparticle cerium and indium oxide exposure. ACS Sustainable Chem. Eng. 1(7), 768–778. https://doi.org/10.1021/sc400098h

Maes, C., Bouquillon, S., Fauconnier, M. L., 2019. Encapsulation of essential oils for the development of biosourced pesticides with controlled release: A review. Molecules 24(14), 2539. https://doi.org/10.3390/molecules24142539.

Medina-Velo, I.A., Zuverza-Mena, N., Tamez, C., Ye, Y., Hernandez-Viezcas, J.A., White, J.C., Peralta-Videa, J.R., Gardea-Torresdey, J.L., 2018. Minimal transgenerational effect of ZnO nanomaterials on the physiology and nutrient profile of *Phaseolus vulgaris*. ACS Sustainable Chem. Eng. 6(6), 7924-7930. https://doi.org/10.1021/acssuschemeng.8b01188.

Miloudi, S., Abbad, I., Soulaimani, B., Ferradous, A., Abbad, A., 2024. Optimization of herbicidal activity of essential oil mixtures from *Satureja alpina*, *Thymus satureioides* and *Myrtus communis* on seed germination and post-emergence growth of *Amaranthus retroflexus* L. Crop Prot. 106642. https://doi.org/10.1016/j.cropro.2024.106642.

Mubeen, I., Mfarrej, M.F.B., Razaq, Z., Iqbal, S., Naqvi, S.A.H., Hakim, F., Mosa, W.F., Moustafa, M., Fang, Y. and Li, B., 2023. Nanopesticides in comparison with agrochemicals: outlook and future prospects for sustainable agriculture. Plant Physio. Biochem. 198, 107670. https://doi.org/10.1016/j.plaphy.2023.107670.

712 Nagy, K., Tessema, R.A., Budnik, L.T., Ádám, B., 2019. Comparative cyto-and genotoxicity
713 assessment of glyphosate and glyphosate-based herbicides in human peripheral white blood
714 cells. Environ Res. 179, 108851. https://doi.org/10.1016/j.envres.2019.108851.
715 Nithiyanantham, U., Zaki, A., Grosu, Y., González-Fernández, L., Anagnostopoulos, A., Navarro,
716 M.E., Ding, Y., Igartua, J.M. and Faik, A., 2022. Effect of silica nanoparticle size on the
717 stability and thermophysical properties of molten salts based nanofluids for thermal energy
718 storage applications at concentrated solar power plants. J. Energy Storage 51, 104276.
719 https://doi.org/10.1016/j.est.2022.104276.
720 Peixoto, S., Henriques, I., Loureiro, S., 2021. Long-term effects of Cu(OH)2 nanopesticide
721 exposure on soil microbial communities. Environ. Pollut. 269, 116113.
722 https://doi.org/10.1016/j.envpol.2020.116113.
723 Perry, E.D., Ciliberto, F., Hennessy, D.A., Moschini, G., 2016. Genetically engineered crops and
724 pesticide use in US maize and soybeans. Sci. Adv. 2(8), e1600850.
725 https://doi.org/10.1126/sciadv.1600850.
726 Pontes, M.S., Antunes, D.R., Oliveira, I.P., Forini, M.M.L., Santos, J.S., Arruda, G.J., Caires,
727 A.R.L., Santiago, E.F., Grillo, R., 2021. Chitosan/tripolyphosphate nanoformulation carrying
728 paraquat: Insights on its enhanced herbicidal activity. Environ. Sci. Nano 8(5), 1336–1351.
729 https://doi.org/10.1039/D0EN01128B.
730 Pouresmaeil, M., Nojadeh, M. S., Movafeghi, A., Maggi, F., 2020. Exploring the bio-control
731 efficacy of *Artemisia fragrans* essential oil on the perennial weed *Convolvulus arvensis*:
732 Inhibitory effects on the photosynthetic machinery and induction of oxidative stress. Ind. Crops
733 Prod. 155, 112785. https://doi.org/10.1016/j.indcrop.2020.112785.
734 Prasad, T., Halder, S., Dhar, S.S., 2020. Process parameter effects on particle size reduction of sol-
735 gel synthesized silica nanoparticles. Materials Today: Proceedings 22, 1669-1675.
736 https://doi.org/10.1016/j.matpr.2020.02.184.
737
738 Qu, R., He, B., Yang, J., Lin, H., Yang, W., Wu, Q., Li, Q.X., Yang, G., 2021. Where are the new
739 herbicides? Pest Manag. Sci. 77, 2620–2625. https://doi.org/10.1002/ps.6285.
740 Raseetha, S., Oey, I., Burritt, D.J., Heenan, S., Hamid, N., 2013. Evolution of antioxidant enzymes
741 activity and volatile release during storage of processed broccoli (*Brassica oleracea* L. italica).
742 LWT Food Sci. Technol. 54, 216–223. https://doi.org/10.1016/j. lwt.2013.05.024.

743 Sarita, Mehrotra S., Dimkpa, C.O., Goyal V. 2023. Survival mechanisms of chickpea (*Cicer*
744 *arietinum*) under saline condition. Plant Physiol. Biochem. 205:108168.
745 Sattary, M., Amini, J., Hallaj, R., 2020. Antifungal activity of the lemongrass and clove oil
746 encapsulated in mesoporous silica nanoparticles against wheat's take-all disease. Pest.
747 Biochem. Physio. 170, 104696. https://doi.org/10.1016/j.pestbp.2020.104696.
748 Scavo, A., Abbate, C., Mauromicale, G., 2019. Plant allelochemicals: agronomic, nutritional and
749 ecological relevance in the soil system. Plant Soil 442, 23–48. https://doi.org/10.1007/s11104-
750 019-04190-y.
751 Shedden K., 2015. Generalized linear models. Department of statistics. University of Michigan.
752 Creative Commons Attribution Share Alike 3.0 License. 35p.
753 Synowiec, A., Lenart-Boroń, A., Bocianowski, J., Lepiarczyk, A., Kalemba, D., 2019. How soil-
754 applied maltodextrin with caraway (*Carum carvi* L.) oil affects weed and soil microbiological
755 activity in maize (*Zea mays* L.) stands. Polish J. Environ. Stud. 29(1), 817-826.
756 https://doi.org/10.15244/pjoes/102365.
757 Taban, A., Saharkhiz, M.J., Khorram, M., 2020. Formulation and assessment of nano-encapsulated
758 bioherbicides based on biopolymers and essential oil. Ind. Crops Prod. 149, 112348.
759 https://doi.org/10.1016/j.indcrop.2020.112348.
760 Takeshita, V., de Sousa, B.T., Preisler, A.C., Carvalho, L.B., Pereira, Ad.E.S., Tornisielo, V.L.,
761 Dalazen, G., Oliveira, H.C., Fraceto, L.F., 2021. Foliar absorption and field herbicidal studies
762 of atrazine-loaded polymeric nanoparticles. J. Hazard. Mater. 418, 126350.
763 https://doi.org/10.1016/j.jhazmat.2021.126350.
764 Tamez, C., Molina-Hernandez, M., Medina-Velo, I.A., Cota-Ruiz, K., Hernandez-Viezcas, J.A.,
765 Gardea-Torresdey, J., 2020. Long-term assessment of nano and bulk copper compound
766 exposure in sugarcane (*Saccharum officinarum*). Sci. Tot. Environ. 718, 137318.
767 https://doi.org/10.1016/j.scitotenv.2020.137318.
768 Torres-Pagán, N., Muñoz, M., Barbero, S., Mamone, R., Peiró, R., Carrubba, A., Sánchez-
769 Moreiras, A.M., Gómez de Barreda, D., Verdeguer, M., 2024. Herbicidal potential of the
770 natural compounds carvacrol, thymol, eugenol, p-cymene, citral and pelargonic acid in field
771 conditions: indications for better performance. Agronomy 14, 537.
772 https://doi.org/10.3390/agronomy14030537.

Travlos, I., Rapti, E., Gazoulis, I., Kanatas, P., Tataridas, A., Kakabouki, I., Papastylianou, P., 2020. The herbicidal potential of different pelargonic acid products and essential oils against several important weed species. Agronomy 10, 1687. https://doi.org/10.3390/agronomy10111687.

United Nations. The world population prospects 2024: highlights. New York: United Nations; 2024. https://population.un.org/wpp/Graphs/DemographicProfiles/Line/900. Accessed 18 August 2024.

Vaidya, S., Deng, C., Wang, Y., Zuverza-Mena, N., Dimkpa, C.O., White, J.C., 2024. Nanotechnology in agriculture: A solution to global food insecurity in a changing climate? NanoImpact 34, 100502. https://doi.org/10.1016/j.impact.2024.100502.

Vendan, S.E., Manivannan, S., Sunny, A.M., Murugesan, R., 2017. Phytochemical residue profiles in rice grains fumigated with essential oils for the control of rice weevil. PLoS ONE, 12(10), p.e0186020. https://doi.org/10.1371/journal.pone.0186020.

Verdeguer, M., Sánchez-Moreiras, A.M., Araniti, F., 2020. Phytotoxic effects and mechanism of action of essential oils and terpenoids. Plants 9, 1571. https://doi.org/10.3390/plants9111571.

Wang, X.D., Shen, Z.X., Sang, T., Cheng, X.B., Li, M.F., Chen, L.Y., Zhan-Shan Wang, Z.S., 2010. Preparation of spherical silica particles by Stöber process with high concentration of tetra-ethyl-orthosilicate. J Colloid Interface Sci. 341, 23-29. https://doi.org/10.1016/j.jcis.2009.09.018.

Yan, X., Cheng, M., Zhao, P., Wang, Y., Chen, M., Wang, X. and Wang, J., 2022. Fabrication and characterization of oxidized esterified tapioca starch films encapsulating oregano essential oil with mesoporous nanosilica. Ind. Crops Prod. 184, 115033. https://doi.org/10.1016/j.indcrop.2022.115033.

Zaid, A., Wani, S.H., 2019. Reactive oxygen species generation, scavenging and signaling in plant defense responses. In *Bioactive molecules in plant defense*: *Signaling in growth and stress* (pp. 111-132). Cham: Springer International Publishing. https://doi.org/10.1007/978-3-030-27165-7_7.

Zainy, Z., Fayyaz, M., Yasmin, T., Hyder, M. Z., Haider, W., Farrakh, S., 2023. Antioxidant enzymes activity and gene expression in wheat-stripe rust interaction at seedling stage. Physio. Molecular Plant Path. 124, 101960. https://doi.org/10.1016/j.pmpp.2023.101960.

Zhang, R., Cui, Y., Cheng, M., Guo, Y., Wang, X. Wang, J. 2021. Antifungal activity and mechanism of cinnamon essential oil loaded into mesoporous silica nanoparticles. Ind. Crops Prod. 171, 113846. https://doi.org/10.1016/j.indcrop.2021.113846

Zhang, Z., Tan, Y., McClements, D. J., 2021. Investigate the adverse effects of foliarly applied antimicrobial nanoemulsion (carvacrol) on spinach. LWT Food Sci. Technol. 141, 110936. https://doi.org/10.1016/j.lwt.2021.110936.

Zhao, C., Liu, B., Piao, S., Wang, X., Lobell, D.B., et al., 2017. Temperature increase reduces global yields of major crops in four independent estimates. Proc. Nat. Acad. Sci. USA. 114(35), 9326–9331. https://doi.org/10.1073/pnas.1701762114.

Zhou S., Han C., Zhang C., Kuchkarova N., Wei C., Zhang C., Shao H., 2021. Allelopathic, phytotoxic, and insecticidal effects of *Thymus proximus* Serg. essential oil and its major constituents. Front. Plant Sci. 12: 689875. https://doi.org/10.3389/fpls.2021.689875.